

Large area mapping of southwestern forest crown cover, canopy height, and biomass using the NASA Multiangle Imaging Spectro-Radiometer

Mark Chopping^{a,*}, Gretchen G. Moisen^b, Lihong Su^a, Andrea Laliberte^c, Albert Rango^c,
John V. Martonchik^d, Debra P.C. Peters^c

^a Department of Earth and Environmental Studies, Montclair State University, Montclair, NJ 07043

^b USDA, Forest Service, Rocky Mountain Research Station, 507 25th Street, Ogden, UT 84401

^c USDA, Agricultural Research Service, Jornada Experimental Range, Las Cruces, NM 88003

^d NASA Jet Propulsion Laboratory, Pasadena, CA 91109

Received 1 November 2006; received in revised form 22 June 2007; accepted 15 July 2007

Abstract

A rapid canopy reflectance model inversion experiment was performed using multi-angle reflectance data from the NASA Multi-angle Imaging Spectro-Radiometer (MISR) on the Earth Observing System Terra satellite, with the goal of obtaining measures of forest fractional crown cover, mean canopy height, and aboveground woody biomass for large parts of south-eastern Arizona and southern New Mexico (>200,000 km²). MISR red band bidirectional reflectance estimates in nine views mapped to a 250 m grid were used to adjust the Simple Geometric-optical Model (SGM). The soil-understory background signal was partly decoupled *a priori* by developing regression relationships with the nadir camera blue, green, and near-infrared reflectance data and the isotropic, geometric, and volume scattering kernel weights of the LiSparse–RossThin kernel-driven bidirectional reflectance distribution function (BRDF) model adjusted against MISR red band data. The SGM's mean crown radius and crown shape parameters were adjusted using the Praxis optimization algorithm, allowing retrieval of fractional crown cover and mean canopy height, and estimation of aboveground woody biomass by linear rescaling of the dot product of cover and height. Retrieved distributions of crown cover, mean canopy height, and aboveground woody biomass for forested areas showed good matches with maps from the United States Department of Agriculture (USDA) Forest Service, with R² values of 0.78, 0.69, and 0.81, and absolute mean errors of 0.10, 2.2 m, and 4.5 tons acre⁻¹ (10.1 Mg ha⁻¹), respectively, after filtering for high root mean square error (RMSE) on model fitting, the effects of topographic shading, and the removal of a small number of outliers. This is the first use of data from the MISR instrument to produce maps of crown cover, canopy height, and woody biomass over a large area by seeking to exploit the structural effects of canopies reflected in the observed anisotropic patterns in these explicitly multiangle data.

© 2008 Elsevier Inc. All rights reserved.

Keywords: Forest; Biomass; Carbon; Canopy; Structure; BRDF; Multiangle; Geometric–optical; model

1. Introduction

Maps of forest canopy parameters are required for a wide range of ecological applications, including the assessment of changing carbon pools and the potential for carbon emissions to the atmosphere, as well as for economic and forest management purposes. In this study, we pursue a multi-angle approach to mapping that seeks to exploit the structural effects of canopies on observed radiation fields in the red wavelengths by fitting the

data to a geometric-optical (GO) canopy reflectance model. This approach potentially provides both upper canopy parameters (fractional crown cover, mean canopy height, aboveground woody biomass) and a measure of understory foliage density and thus has important applications in mapping the changing structure of forests and fire fuel loads. This is important because the effects of recent climate change on western forests are now being witnessed (Running, 2006). Westerling et al. (2006) found that in the period 1970–2003, the length of the active wildfire season in the western US increased by 78 days and that the average burn duration of large fires increased from 7.5 to 37.1 days. This dramatic change in

* Corresponding author.

E-mail address: chopping@pegasus.montclair.edu (M. Chopping).

wildfire activity is attributed to an increase in spring and summer temperatures by ~ 0.9 °C and a one- to four-week earlier melting of mountain snowpacks. High-elevation forests between 1680 m and 2690 m that were previously protected from fire by late snowpacks are becoming increasingly vulnerable. An increased frequency of forest fires over greater extents and of longer durations will result in much greater losses of carbon to the atmosphere; wildfires add an estimated 3.5×10^{15} g to atmospheric carbon emissions each year, or roughly 40% of fossil fuel carbon emissions (Running, 2006).

Remote sensing from satellite altitudes has long been used to map forest type and cover and there is an increasing need to produce and distribute maps of numerous forest attributes over large geographic areas in a rapid fashion. As well as providing spatially contiguous estimates of C pools and emissions to the atmosphere from wildfires, other important applications of these maps include assessing the status of suitable wildlife habitat; accounting for forest resources affected by fire; quantifying the effects of urbanization; identifying land suitable for timber harvest; and locating areas at high risk for plant invasions, and insect or disease outbreaks. However, in addition to the non-trivial requirement for radiometric calibration and correction for atmospheric attenuation of the signal, spectral radiance measurements from orbiting instruments must be calibrated and validated against field reference data. The US Forest Service (USFS), Forest Inventory and Analysis Program (FIA) collects a systematic sample of field data across all ownerships in the US. These plot data are used together with those from NASA's Moderate Resolution Imaging Spectro-Radiometer (MODIS) and other data in a modeling framework to map important forest canopy parameters over large areas. The approach involves the use of reflectance bands from three eight-day image composites, vegetation indices (Normalized Difference Vegetation Index, and Enhanced Vegetation Index) from three 16-day composites, percent tree cover from the MODIS Vegetation Continuous Fields (VCF) (Hansen et al., 2003), and the fire occurrence product (US Forest Service, 2005). These data have been combined with those on elevation, slope, aspect, soils, existing ecoregion and land cover maps, and climate (temperature and precipitation minima, maxima, and averages) in predictive non-parametric models of forest attributes (e.g., Blackard & Moisen, 2005; Ruefenacht et al., 2004).

While the spectral and temporal information available from wide-swath moderate resolution remote sensing has proved extremely valuable in constructing new maps of forest attributes over regional or global areas that could not be produced in any other way, some limitations have been recognized. First, canopy structural measures are less straightforward to estimate because spectral measures capture structural effects only indirectly: spectral remote sensing data rely mainly on the optical properties of vegetation and soil elements (spectral reflectance, absorption and transmittance). Second, there are limits on how well the empirical regression tree methods used can predict tree cover given the spectral confusion of different cover types. The VCF product that employs these algorithms has been tested against forest plot data from two independent ground-based tree cover databases (White et al., 2005): the United States Forest

Service (USFS) Forest Inventory Analysis (FIA) database (1176 plots for Arizona) and the Southwest Regional GAP data base (SWReGAP; 2778 plots for Utah and western Colorado). Overall RMS error was 24% for SWReGAP and 31% for FIA data. The study also showed that bias in the VCF product was positive for low tree cover, but systematically became increasingly negative with tree cover until at $>60\%$ the VCF tree cover underestimated the observed tree cover by 40% and 45% vs. SWReGAP and FIA data sets, respectively. Note that the VCF is a global product with multiple layers that covers all land areas at a resolution of 500 m.

An alternative approach that may be highly complementary to the spectral methods used hitherto is to exploit spectral radiance measurements by a multiangle instrument such as the NASA/JPL Multi-angle Imaging Spectro-Radiometer (MISR) and use a simple geometric–optical canopy reflectance model to characterize the forest canopy reflectance anisotropy. While it is possible to adopt empirical and data-mining methods, or complex radiative transfer models, simplified models have the advantage over the former in that they have greater explanatory power (the physical validity and consistency of internal parameters can be checked), and the advantage over the latter in that they are able to resolve statistical distributions of discrete objects within the instrument field-of-view (IFOV) (Strahler et al., 2005). Simple geometric–optical (GO) models treat the surface as an assemblage of discrete objects of equal radius, shape and height, evenly distributed within a spatial unit. A tree or shrub crown is represented by a geometric primitive (e.g., spheroid, cone, or cylinder) whose center is located at a specified mean height above a (nominally diffuse scattering) background. These models predict the top-of-canopy reflectance response to important canopy biophysical parameters (plant number density, foliage volume, mean canopy crown height and radius, crown shape, understory density, and soil characteristics) as a linear combination of the contributions from sunlit and viewed, and shaded and viewed components (Chen et al., 2000; Li & Strahler, 1985), as in Eq. (1):

$$R = G \cdot k_G + C \cdot k_C + T \cdot k_T + Z \cdot k_Z. \quad (1)$$

Where R is bidirectional spectral reflectance; k_G , k_C , k_T and k_Z are the GO modeled proportions of sunlit background, sunlit crown, shaded crown and shaded background, respectively; and G , C , T , and Z are the contributions of the sunlit background, sunlit crown, shaded crown, and shaded background, respectively. GO models are particularly appropriate for the exploitation of solar wavelength remote sensing data acquired at differing viewing and/or illumination angles because the proportions of sunlit and shaded crown and background in the remote sensing instrument ground-projected IFOV vary with both viewing and illumination angles and thereby reveal the canopy structure.

2. Methods

The study area encompasses parts of south-eastern Arizona and southern New Mexico ($>200,000$ km²) that includes desert

grassland (often with significant woody shrub encroachment); riparian and river valley woodland along the Rio Grande, San Pedro, Salt, and Gila rivers; and upland forest (including the Coronado, Lincoln, Cibola, Apache, Sitgreaves, and Tonto National Forests, and the Gila National Forest and Wilderness (Fig. 1). The major tree species include cottonwood (*Populus fremontii*, *P. wislizeni*) and salt–cedar (*Tamarix* spp.) in riparian and river valley environments and pinyon (*Pinus* subsection *Cembroidesa*), juniper (*Juniperus* spp.), Douglas–fir (*Pseudotsuga menziesii*), ponderosa pine (*Pinus ponderosa*), lodgepole pine (*Pinus contorta*), Engelmann spruce (*Picea engelmannii*), aspen (*Populus tremuloides*), and oak (*Quercus* spp.) in the higher elevations. In the desert grassland regions major woody species include creosotebush (*Larrea tridentata*), honey mesquite (*Prosopis glandulosa*), and tarbush (*Flourensia cernua*).

This study used three MISR data products: the MISR level 1B2 MI1B2T Terrain-projected Spectral Radiance product; the MISR Level 1B2 MI1B2GEOP Geometric Parameters product; and the MISR Level 2 MIL2ASAE Aerosol product. The MI1B2T product is the terrain-projected top-of-atmosphere spectral radiance with a nominal 1.1 km spatial resolution in the off-nadir, non-red bands and a nominal 275 m spatial resolution in the nadir multispectral and off-nadir red bands (Diner et al., 1999). The MI1B2GEOP product provides grids of solar azimuth, solar zenith, and nine viewing azimuth and zenith angles at 17.6 km resolution. The MIL2ASAE product provides regional mean spectral optical depth at 558 nm with 17.6 km resolution. These data from MISR were acquired for twelve

Terra satellite overpasses in late May and early June 2002, covering a period of one month, as follows:

- path 033: 013039 (2002-05-31), 012806 (2002-05-15), and 013272 (2002-06-16)
- path 034: 013141 (2002-06-07), 012675 (2002-05-06), and 013374 (2002-06-07)
- path 035: 013010 (2002-05-29), 013243 (2002-06-14), and 013476 (2002-06-30)
- path 036: 013112 (2002-06-05), 012646 (2002-05-04), and 013345 (2002-06-21)

This period represents the end of the dry season and was selected for maximum woody plant greenness versus graminoid greenness (i.e., with largely senescent grasses), and for lower cloud cover. In addition, surface conditions are unlikely to change importantly in this semi-arid environment that this time of year. MISR consists of nine pushbroom cameras that acquire image data with nominal view zenith angles relative to the surface reference ellipsoid of 0.0° , $\pm 26.1^\circ$, $\pm 45.6^\circ$, $\pm 60.0^\circ$, and $\pm 70.5^\circ$ (forward and aft of the Terra satellite) in four spectral bands (446, 558, 672, and 866 nm). The 672 nm (red) band images are acquired with a nominal maximum crosstrack ground spatial resolution of 275 m in all nine cameras and all bands are acquired at this resolution in the nadir camera (Diner et al., 1999). The MISR spectral radiance data were corrected for atmospheric absorption and scattering using the Simplified Method for Atmospheric Correction (SMAC) algorithm (Rahman & Dedieu,

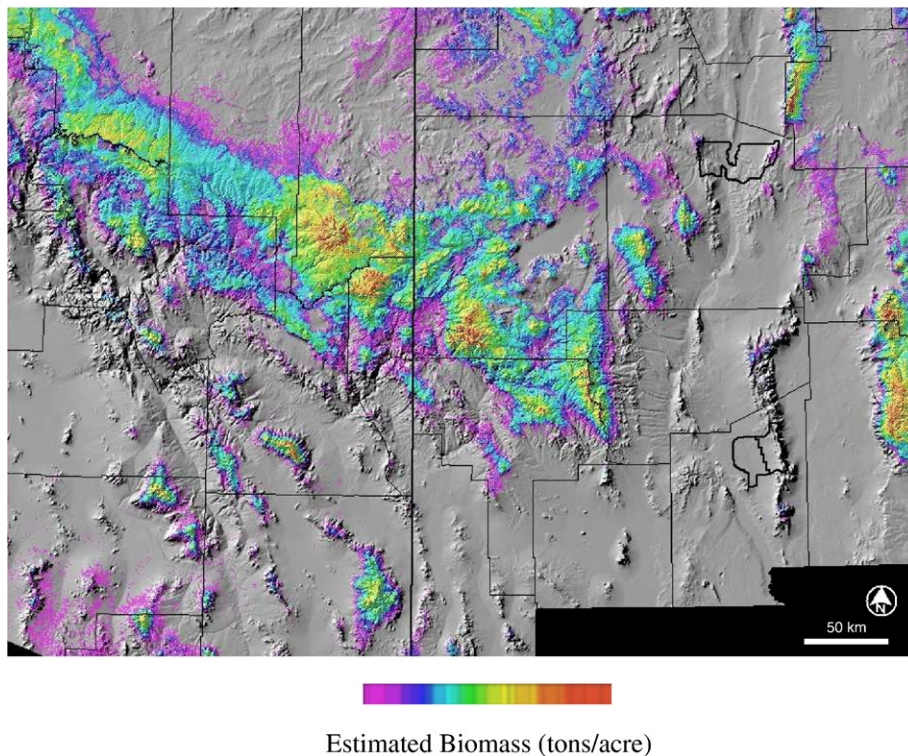


Fig. 1. US Forest Service forest biomass map of the study area, draped over a hillshade layer. The thick solid vertical line is the Arizona/New Mexico border; thin lines indicate county boundaries. The two polygons delineated in thick lines show, from south to north, the locations of the USDA, ARS Jornada Experimental Range and the Sevilleta National Wildlife Refuge, respectively. White Sands National Monument lies between the Range and the Sacramento Mountains to the east.

1994), version 4 and MISR estimates of aerosol optical depth. A kriging method was used to smooth the MISR 17.6 km aerosol optical depth data prior to application in the estimation of surface bidirectional reflectance factors. The data were then resampled using bilinear interpolation to the Universal Transverse Mercator map projection, WGS84 spheroid/datum, zones 12 and 13, with a grid interval of 250 m, chosen for compatibility with MODIS imagery and the mapped reference data.

The simple geometric model (SGM), a GO model incorporating a dynamic background and a crown volume scattering term, was used (Chopping et al., 2006, 2008). It is formulated as Eq. (2):

$$R = G_{\text{Walthall}}(\vartheta_i, \vartheta_v, \varphi) \cdot k_G(\vartheta_i, \vartheta_v, \varphi) + C_{\text{Ross}}(\vartheta_i, \vartheta_v, \varphi) \cdot k_C(\vartheta_i, \vartheta_v, \varphi) \quad (2)$$

where ϑ_i , ϑ_v and φ are the view zenith, solar zenith and relative azimuth angles, respectively; k_G and k_C are the calculated proportions of sunlit and viewed background and crown, respectively; G_{Walthall} is the background contribution from the modified Walthall model (Nilson & Kuusk, 1989; Walthall et al., 1985); and C_{Ross} is the simplified Ross turbid medium approximation for plane parallel canopies (Ross, 1981). The shaded components T and Z (Eq. (1)) are discarded; they are assumed black, as in the kernel-driven bidirectional reflectance distribution function (BRDF) models (Roujean et al., 1992; Wanner et al., 1995). k_G and k_C are calculated exactly via Boolean geometry for the principal and perpendicular planes and approximated away from these; they are provided by Eqs. (3) and (4), respectively:

$$k_G = e^{-\lambda\pi^2\{\sec\vartheta'_i + \sec\vartheta'_v - O(\vartheta_i, \vartheta_v, \varphi)\}} \quad (3)$$

$$k_C = \left(1 - e^{-\lambda\pi^2\sec\vartheta'_v}\right) \frac{1}{2}(1 + \cos\varepsilon') \quad (4)$$

where λ is the number density of objects; r is the average radius of these objects; and O is the overlap area between the shadows of illumination and viewing (Wanner et al., 1995); Eq. (5):

$$O = 1/\pi(t - \sin t \cos t)(\sec\vartheta'_i + \sec\vartheta'_v) \quad (5)$$

where t is a parameter that indirectly expresses the locations of the end points of the line that intersects the shadows of viewing and illumination. This allows k_G to be expressed in a way that depends only on the value of t (Wanner et al., 1995). All these functions include the parameters b/r (vertical crown radius/horizontal crown radius) and h/b (height of crown center/vertical crown radius) which describe the shape and height of the crown. The prime indicates equivalent zenith angles obtained by a vertical scale transformation in order to treat spheroids as spheres (i.e., $\vartheta' = \tan^{-1}(b/r \tan \vartheta$; Wanner et al., 1995). ε' is the transformed scattering phase angle given by Eq. (6):

$$\cos\varepsilon' = \cos\vartheta'_i \cos\vartheta'_v + \sin\vartheta'_i \sin\vartheta'_v \cos\varphi \quad (6)$$

The model's parameters are plant number density (λ), mean crown radius (r), crown vertical to horizontal radius ratio (b/r),

crown center height to vertical radius ratio (h/b), and crown leaf area index (LAI). Leaf reflectance in the red wavelengths is fixed at 0.09.

To estimate the brightness and shape of the background response, linear multiple regression at a number of calibration sites was used, the independent variables being the LiSparse–RossThin BRDF model isotropic (*iso*), geometric (*geo*), and volume scattering (*vol*) kernel weights plus the blue (B), green (G), and near-infrared (NIR) BRFs from the MISR *An* (nadir-viewing) camera (Chopping et al., 2006, 2008). The kernel weights were obtained by adjusting the LiSparse–RossThin BRDF model against MISR red band bidirectional reflectance factors (BRFs) in all nine cameras using the Algorithm for Modeling Bidirectional Reflectance Anisotropies of the Land Surface (AMBRALS) code (Strahler et al., 1996), with the objective the minimization of absolute Root Mean Square Error (RMSE). The background calibration sites were located in the western part of the USDA Agricultural Research Service (ARS) Jornada Experimental Range and included remnant black grama (*Bouteloua eriopoda*) grassland with honey mesquite (*Prosopis glandulosa*) encroachment, grass-shrub transition zones, and well-established mesquite shrubland with large plants. Regression equations were established for a range of grassland and shrubland canopy/background configurations by setting mean shrub radius and number density extracted from one meter panchromatic Ikonos imagery; fixing the LAI, h/b and b/r model parameters at 2.08, 2.00 and 0.20, respectively (typical values); and using an optimization algorithm to determine the optimal Walthall model parameters with respect to the MISR data. This allowed the regression of each of the four Walthall model parameters on the six independent variables. In this way, *a priori* estimates of the background response were obtained prior to fitting the SGM model to MISR data (Chopping et al., 2008). The Walthall model is used for the background as it is an empirical model capable of describing a very wide range of surfaces; other models – including

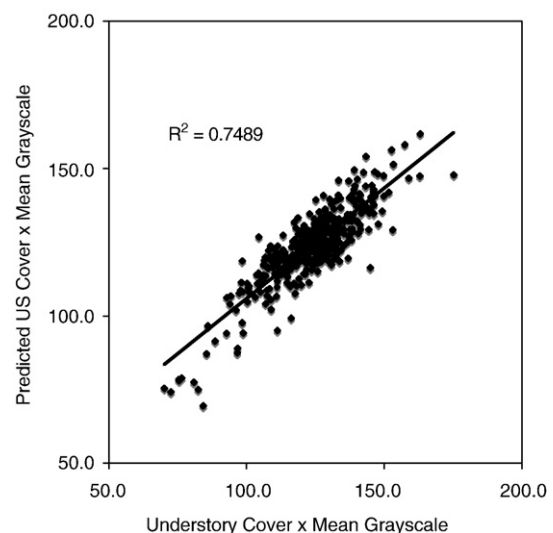


Fig. 2. Predicted background response as a function of the dot product of understory cover and mean understory brightness estimated from one meter panchromatic Ikonos imagery.

semi-empirical models – could also be used. Performance of the soil-understory background estimation method was assessed by using the independent variables to estimate a surrogate of understory density (understory fractional cover \times mean understory grayscale values). The results were reasonable, with an R^2 of 0.75 (Fig. 2). Since the background was derived empirically and with the goal of allowing GO model operation over desert grasslands with shrub encroachment rather than forest, it is expected that some degree of extrapolation error will be incurred over larger geographic regions; this is a first approximation.

The geographic distributions of the background brightness and anisotropy (functions of soil BRDF and understory density) encapsulated in the Walthall model's first (constant) and successive coefficients, respectively, are shown in Fig. 3a–d. It can be seen that the predicted background reflectance (understory density) is lower (higher) in upland areas and along river valleys. Environments in the vicinity of rivers that support significant tree cover are predicted to be quite bright (low understory density) and this is not reasonable. Erroneous predictions are also seen for the very bright alkali flats and gypsum dunes of White Sands National Monument, and for the large lava flow in the eastern part of the area. Also notable are clouds and their shadows and discontinuities at the boundaries where data from different orbital paths are used. The second Walthall model coefficient also shows these discontinuities but the third and fourth Walthall model coefficients have much smoother distributions. Note that these coefficients are for a test data set using one orbit per swath and not those selected in the compositing procedure that produced the final data set.

The SGM was adjusted against the MISR red band data in nine views using the Praxis algorithm (Brent, 1973; Powell, 1964) with $\min(|\text{RMSE}|)$ as the objective function and no weighting of the error terms or constraints imposed. The LAI, λ , and h/b model parameters were fixed at 2.08, 0.012, and 2.00, respectively, with r and b/r left as free parameters set to initial values of 0.25 and 0.2. The routines proceed for each orbital data set by reading from the input data files (multi-angle red reflectance, kernel weight, and nadir camera files), submitting these to the Praxis minimization code that fits the model to the MISR data, and accumulating the results in an output file. The inversions were performed extremely rapidly, completing data from nine orbits in under 12 h running under MacOS X (Unix) on a dual 2.7 GHz G5 Apple Macintosh. Tests showed that it is not possible to retrieve reliable mean plant radius (r) and mean canopy height (h) simultaneously; it is likely that these variables are confounded. When r and b/r were left as free parameters, the results were more reasonable. If λ is fixed (as here) and r is adjusted, this is equivalent to retrieving fractional crown cover. Similarly, if h/b is fixed and b/r is adjusted, this allows the retrieval of an estimate of h , since r and b/r are known (note that h refers to the height of the center of the crown; the height of the top of a tree would be $h+b$). Since the r values retrieved are those that provide the best match with fractional crown cover with a fixed value for λ , some error in the calculated h values is expected.

Note that the coupling of r and b/r in the model means that there is the possibility that these parameters will interfere with each other. However, it would be reasonable to expect that it

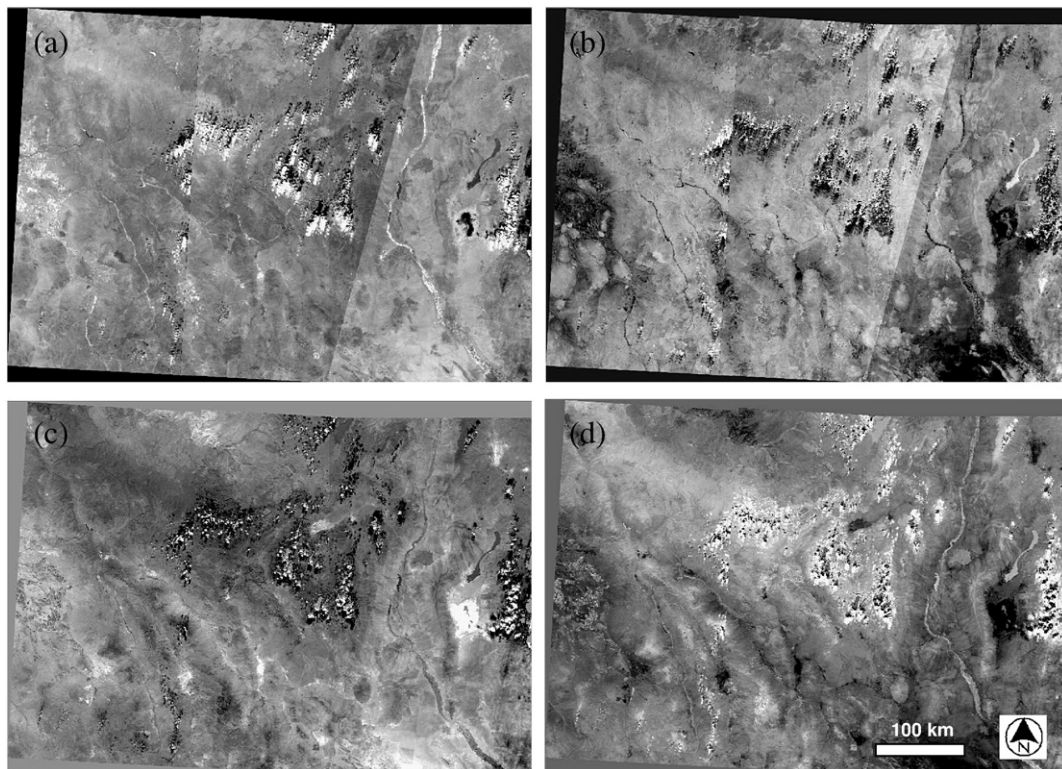


Fig. 3. Maps of background reflectance magnitude (first Walthall model parameter, a surrogate of understory density) and anisotropy (subsequent Walthall model parameters).

might be possible to extract both parameters simultaneously if their respective effects on observed data patterns differ. This does indeed seem to be the case as increasing r is equivalent to increasing fractional cover (which mainly leads to a darkening for all viewing angles with a relatively small change in shape), while increasing b/r results in a stronger change in the degree of observed anisotropy in the MISR plane (Fig. 4) at overpass time (solar zenith angle of $\sim 24^\circ$; relative azimuths in the range $21\text{--}153^\circ$). It is therefore possible to hypothesize that adjusting r allows control over horizontal canopy dimensions while adjusting b/r (effectively, b , since r is also adjustable) allows control over vertical canopy dimensions. Retrievals were thus effectively for fractional woody plant cover, a function of plant number density (fixed) and mean crown radius (adjustable), and mean canopy height, a function of mean crown height (fixed) and mean crown shape (adjustable). An estimate of aboveground woody biomass was made – in a first and perhaps somewhat gross approximation – via linear regression on the dot product of fractional woody cover and mean crown height.

Two sets of model inversions corresponding to two stages in this research were performed. The first set (the “test set”) used data from only one Terra overpass for each MISR swath. This allowed a first test of the method with respect to model fitting and relationships to the reference data but the results contained

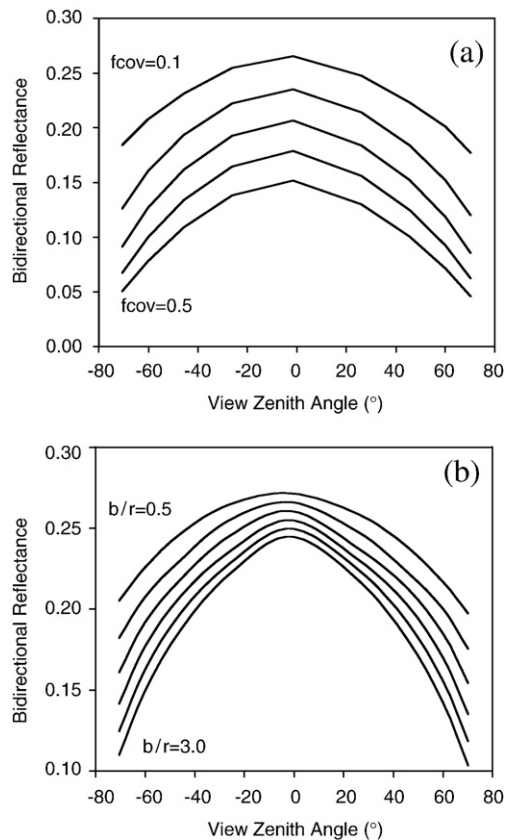


Fig. 4. The modeled effects of: (a) changing fractional crown cover ($fcov$) derived from the retrieved r values, with fixed λ and maintaining canopy height at 3.0 m (b) changing crown shape (b/r) with fixed h/b and background. The LAI, λ , and h/b model parameters were fixed at 2.08, 0.012, and 2.00, respectively. The azimuthal plane corresponds to typical MISR viewing and illumination configurations at this latitude.

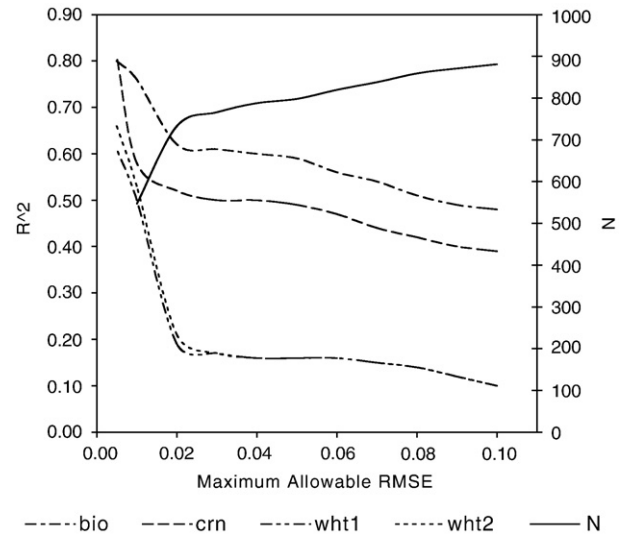


Fig. 5. Effects of filtering on the coefficient of determination (R^2) and the number of data points retained in the test data set (bio=biomass, crn=crown cover, wht1 and wht2=weighted heights).

important cloud and cloud-shadow contamination that was visible in the maps, as well as contamination from topographic shading. To remove poorly illuminated locations, a hillshaded map was constructed for the prevailing illumination conditions using digital elevation data from the Shuttle Radar Topography Mission (SRTM) and a threshold of 0.7 was applied. The second set (the “final set”) used data from 12 overpasses and this additional filtering to remove topographic contamination, with the study area largely accounted for by data from nine MISR overpasses corresponding to three per MISR path. For comparison with reference data, the retrieved parameters were extracted for the same randomly located points in both cases.

Data extracted from USFS raster maps with a spatial resolution of 250 m for the Interior West (IW) produced using FIA data (hereafter IW-FIA) were used as the reference (US Forest Service, 2005). These data are deemed to be more useful than those from the global VCF map of % tree cover because they include many canopy variables and were produced using a modeling framework that relies mainly on FIA survey data, soils, topographic, MODIS vegetation index, VCF, and climate variables (Blackard & Moisen, 2005; Ruefenacht et al., 2004). Disney and Lafont (2004) found that the VCF % tree map overestimates forest cover in the United Kingdom by a factor of almost two with respect to the UK Forestry Authority forest inventory, with better agreement at higher observed forest cover and severe over-estimation for low observed forest cover (only when the VCF % tree cover map for the UK was filtered so that 55% of the data were retained was a close match with UK Forestry Authority data obtained). These results concur with those of White et al. (2005) discussed above. Disney and Lafont (2004) suggest that the root cause of error in the VCF map may be spectral confusion between classes and/or differences between class definitions. They also advocate the use of structural information, through active sensing (radar, lidar) or through multiangle imaging, where the spectral information is not sufficient (Diner et al., 2005). It should be noted that the USFS IW-FIA maps were not intended for validation purposes; the

metadata document (US Forest Service, 2005) that accompanies the geospatial data products created in 2005 by the Interior West region of the Forest Inventory and Analysis Program states that: “The version of this dataset is a draft, intended for review by FIA and other interested parties. The release of this dataset is not intended for use beyond these purposes.” However, these data sets are the most comprehensive and extensive contiguous geospatial data available.

To assess the retrievals with respect to the IW-FIA maps, 4000 randomly located points were selected for the entire area

and only those corresponding to forested areas were extracted, leaving 1063 points. A further 106 (about 10%) of locations were removed because these corresponded to unreasonable parameter values (zero and unphysical high values and outliers where the fractional cover values were more than two standard deviations from the mean). The RMSE on model fitting was then used to further filter the data. The retrieved distributions from the test set were assessed at varying levels of stringency with respect to RMSE and a threshold of 0.01 was applied. Fig. 5 shows, for the test data set, the effects of imposing a more stringent criterion

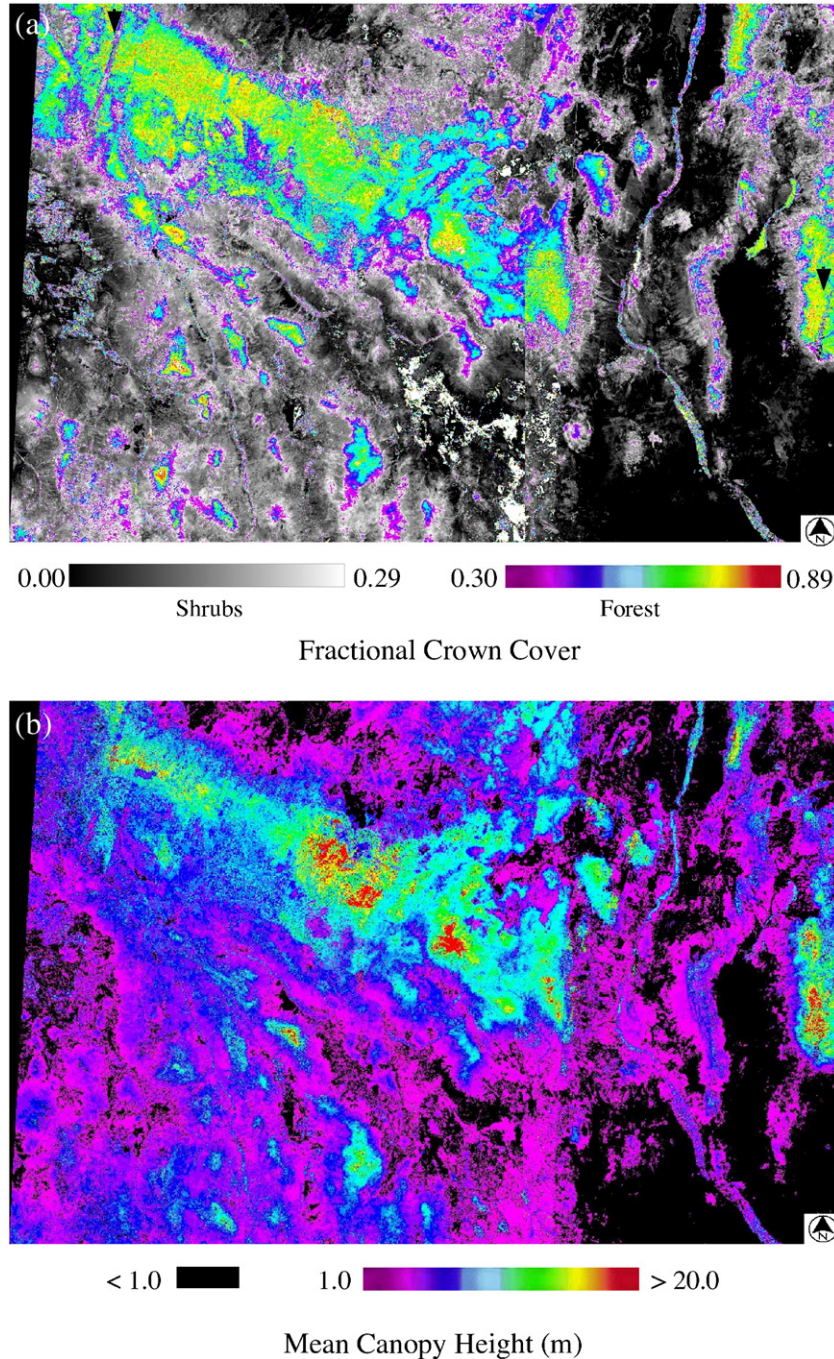


Fig. 6. Maps of (a) fractional crown cover (b) mean canopy height (c) aboveground woody biomass and (d) RMSE on model fitting. Areas in grayscale in (a) and (c) are non-forest; pure white in (a) indicates poor model fitting; arrows in (a) indicate two edge-of-swath anomalies. Grayscale in (d) indicates RMSE < 0.01.

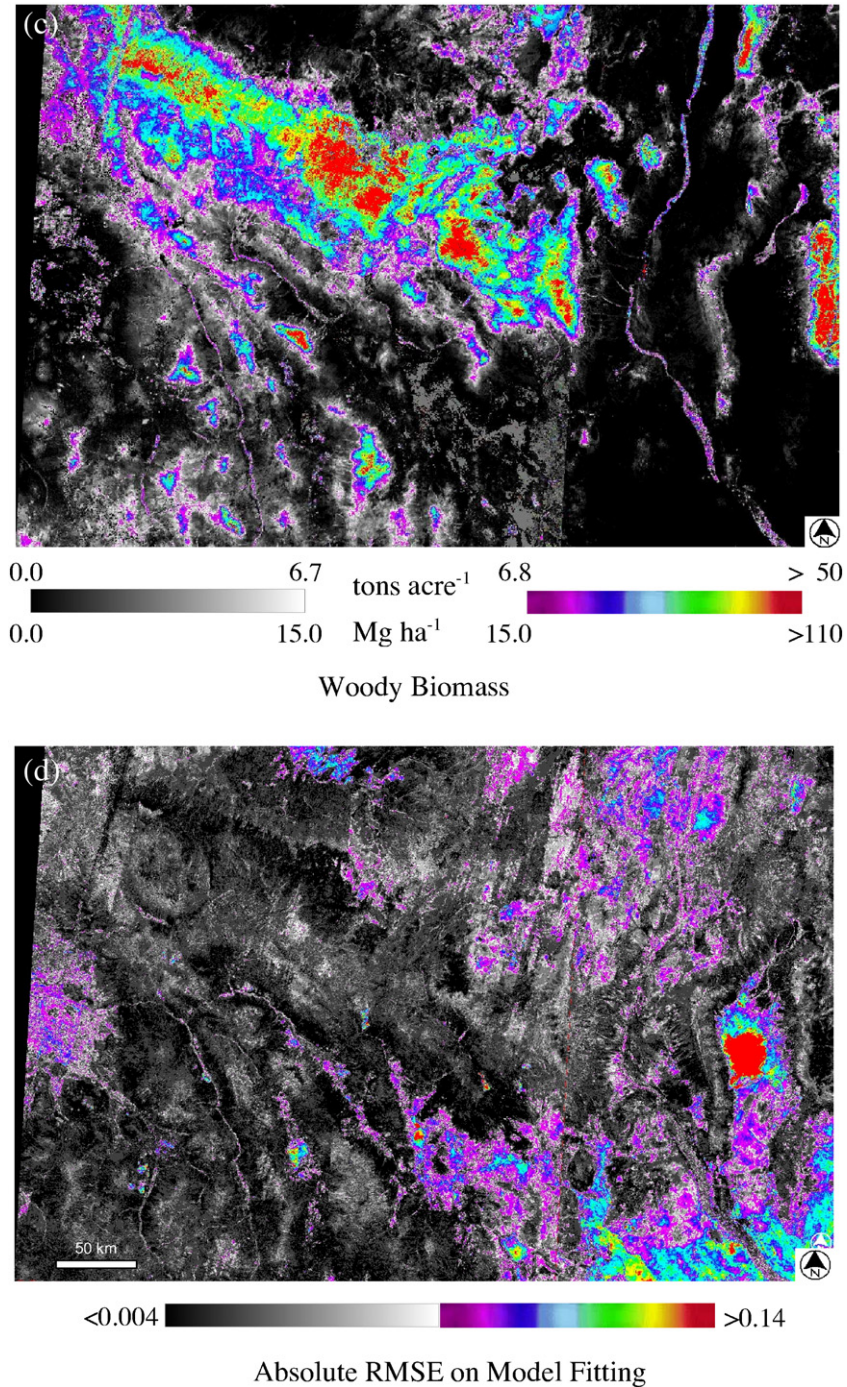


Fig. 6 (continued).

on the coefficient of determination (R^2) for crown cover, woody biomass, and mean canopy height, and the number of remaining data points. Data were extracted for the same 1063 points for the final set and an additional filter was applied to remove results contaminated by topographic shading. The effects of this shading can be clearly seen in the extracted cover data: there is a discrete division between the clusters of affected and unaffected data (Fig. 9a). The filtering for poor model fitting, outliers, and topographic shading resulted in retention of 576, or 54%, of the original 1063 points.

3. Results and discussion

Maps of retrieved woody biomass, fractional crown cover and mean canopy height values and RMSE are shown in Fig. 6. The retrieved parameters exhibit distributions that are similar to existing map products, notably the USFS IW-FIA forest maps (Blackard & Moisen, 2005) and the MODIS Vegetation Continuous Fields (VCF) % tree cover maps (Hansen et al., 2003; not shown). This is perhaps not surprising because all are based at least partly on brightness in the satellite signal: dense

Table 1
Statistics for the final data set

	RMSE	Crown Radius (m)	b/r ratio	Fractional crown cover	Mean canopy height (m)	Woody Biomass	
						(ton acre ⁻¹)	(Mg ha ⁻¹)
Min	0.000	2.15	0.23	0.16	1.37	5.8	12.9
Max	0.010	7.61	4.39	0.89	46.08	98.1	219.9
Mean	0.006	4.20	1.20	0.48	10.34	21.8	49.0
S.D.	0.002	0.96	0.38	0.15	5.04	13.0	29.1
Mean +2 S.D.	0.008	5.16	1.58	0.63	15.38	34.8	78.1
Mean -2 S.D.	0.004	3.24	0.82	0.33	5.29	8.9	19.9

forest is darker than sparse forest or open shrubland. There are many instances for which the inversions failed or produced erroneous results. These include those where it was not possible

to fit the model to the observed data well, resulting in a high RMSE; those where the background response was poorly estimated, resulting in erroneous predictions of no woody plant

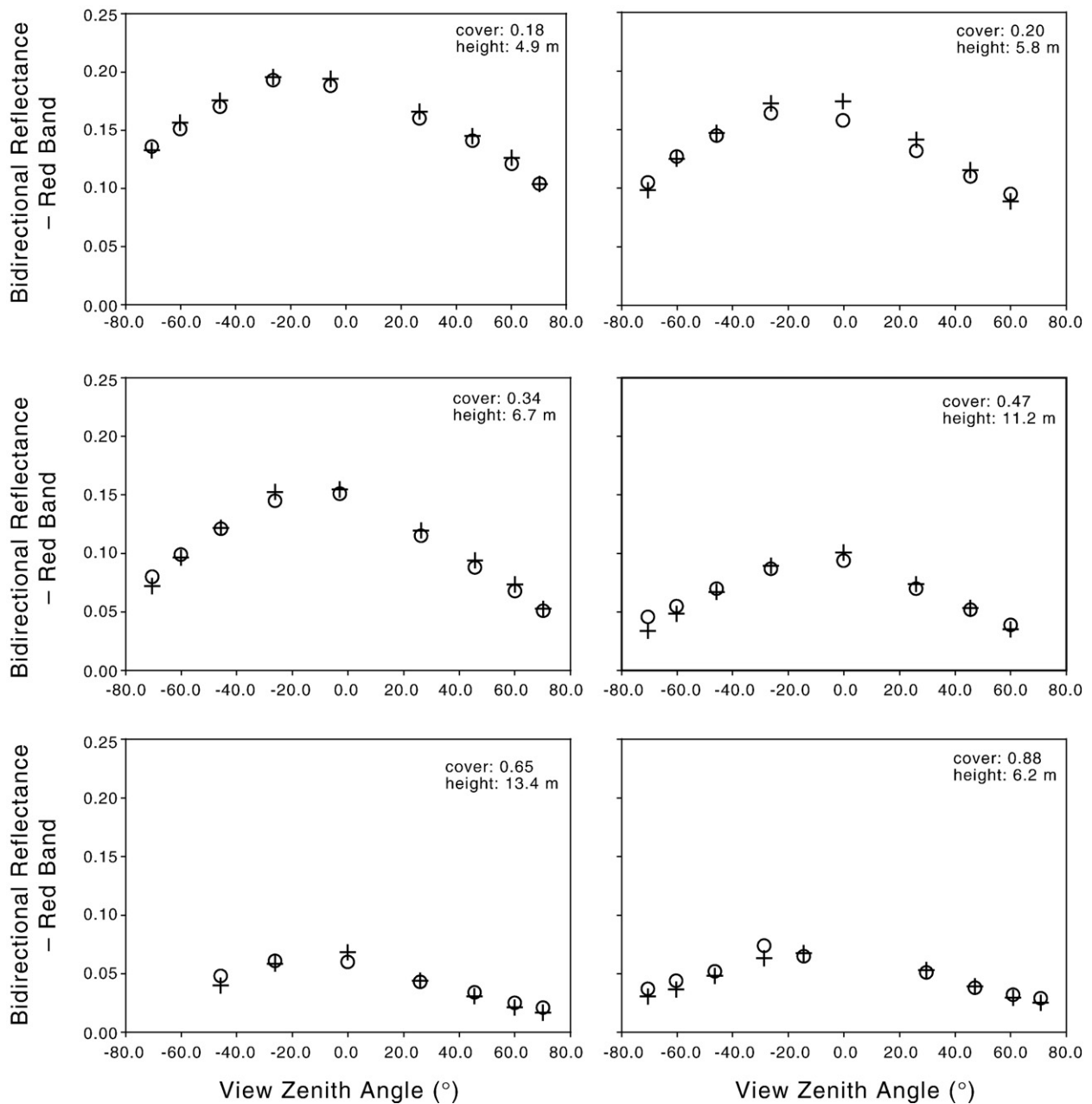


Fig. 7. SGM fits to MISR red band data corresponding to selected comparison points, for a range of forest crown cover values, O=MISR+=SGM.

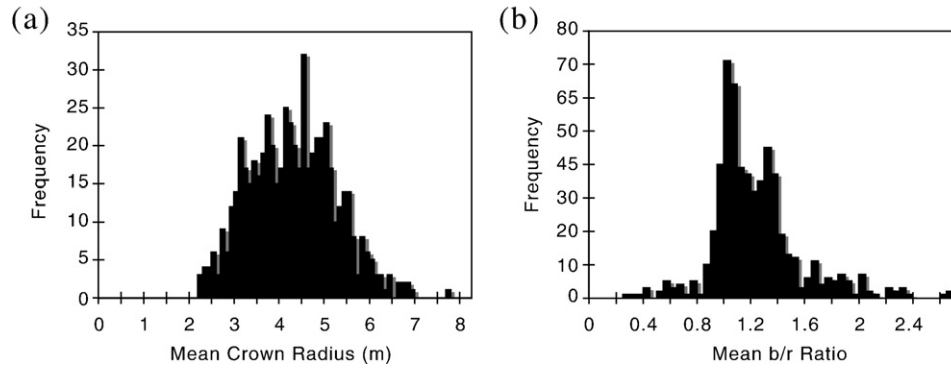


Fig. 8. Frequency distributions for the retrieved and filtered r and b/r model parameters.

cover for some sparse locations (e.g., missing mesquite shrubs south of White Sands National Monument, which appears with very high RMSE in Fig. 6d); and those where retrievals were compromised because of specific isolated surface features (lava flows, lakes, rivers). For low- or no-cover and erroneous retrievals, the output was flagged by setting to zero (black) or one (white) in the fractional cover map (Fig. 6a). Anomalous cover values were also seen where swaths are stitched or because of residual atmospheric and cloud contamination of the signal that is not accounted for in the atmospheric correction:

even though clouds are very sparse in this semi-arid region at the end of the dry season, the contrails of commercial jet aircraft may be persistent and there is also the possibility of important desert dust entrainment into the atmosphere. The quality of fits to observations (i.e., RMSE) can be used to gauge the validity of and to filter the retrieved data, reducing the impact of these anomalies.

For the final data set, the mean and standard deviation of RMSE on model fitting (composited but unfiltered, for all locations) were 0.012 and 0.025, with the vast majority of inversions providing

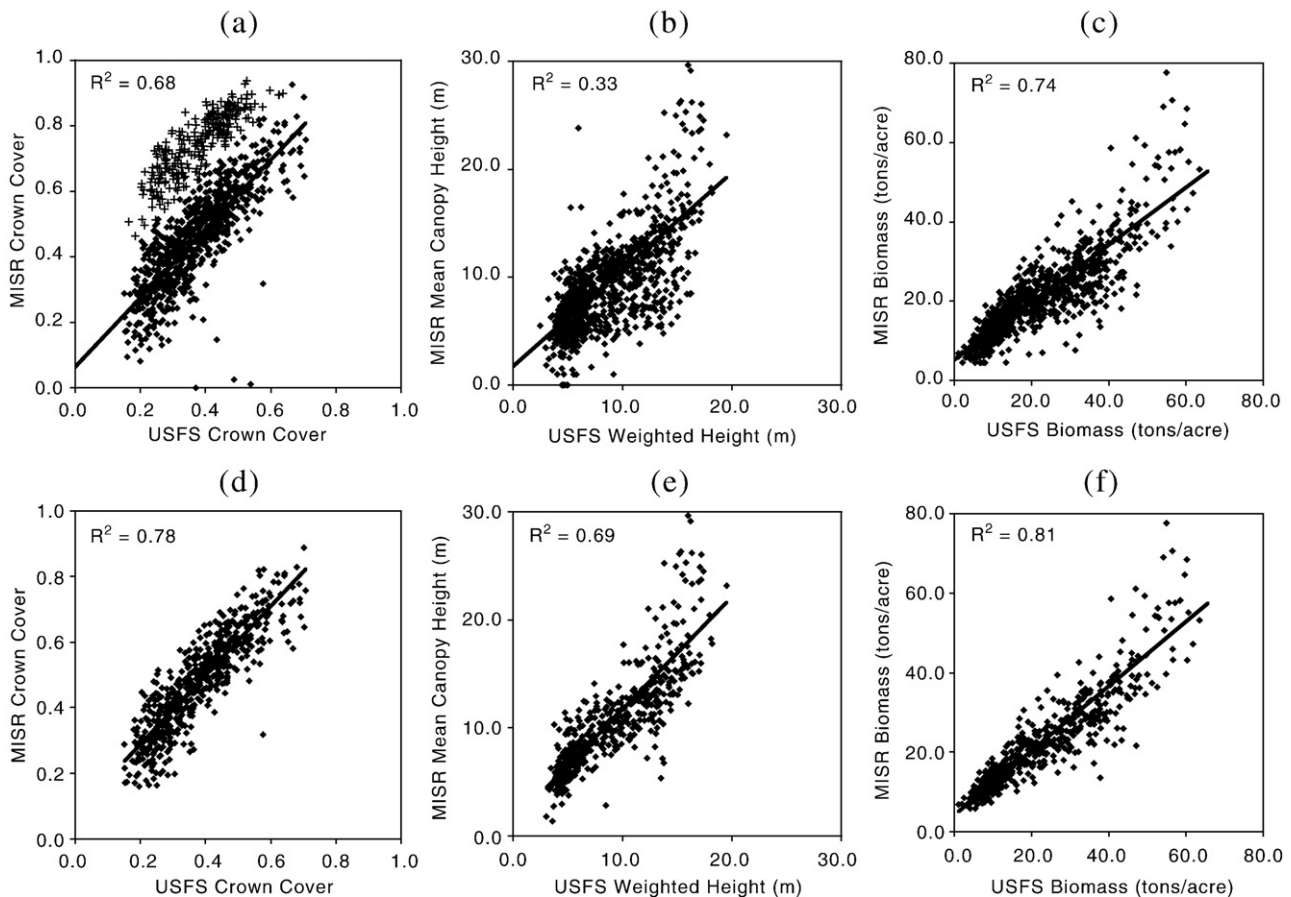


Fig. 9. Filtered inversion results: retrievals of fractional crown cover, mean canopy height, and woody biomass plotted against reference data extracted from the USFS IW-FIA maps, with no restriction on RMSE: (a) woody biomass (b) crown cover (c) mean canopy height; and with filtering: (d) woody biomass (e) crown cover (f) mean canopy height. The cluster of data points indicated by + in (a) corresponds to retrievals contaminated by topographic shading.

RMSE < 0.015 and a mode of 0.004. Table 1 provides a summary of results for the extracted data (N = 576). The mean and standard deviation of RMSE for the extracted final data set used for comparison with the IW-FIA data were 0.006 and 0.002 with a mode of 0.005. The extent of the area for which RMSE was < 0.01 is indicated in Fig. 6d. This covers almost all forest areas. SGM fits to MISR red band data for a range of fractional crown cover values from locations corresponding to comparison points show good agreement (Fig. 7).

Retrieved fractional crown cover and mean canopy height ranged from 0.16–0.89 and 1.4–46 m, respectively, while estimated woody biomass ranged from 5.8–98.1 ton acre⁻¹ (12.9–219.9 Mg ha⁻¹). Since the mapped parameters are calculated from mean crown radius (r) and mean crown shape factor (b/r), it is important to assess whether the model's internal parameters are reasonable, i.e., whether the inversions were well behaved. If they are not then the results might be spurious. The spatial distribution of retrieved mean crown radius values matches that of fractional cover (Fig. 6a) and the range of values for the sample points (post-filtered) is 2.1 m to 7.6 m with a unimodal, quasi-normal distribution centered on a mean of 4.2 m (Fig. 8a). The spatial distribution of crown shape factors (b/r ratio values) largely follows that of the IW-FIA weighted height map (not shown). The distribution of b/r values for the sample points (post-filtered) has a range of 0.22 (oblate; typical for shrubs) to 4.39 (prolate; typical for coniferous trees) and is weakly bimodal, with a quasi-normal distribution centered on 1.20 (slightly prolate crowns; Fig. 8b). The spatial arrangements, ranges and frequency distributions of the retrieved r and b/r parameters thus seem quite reasonable. The retrieved fractional crown cover, woody biomass, and mean canopy height values were plotted against the corresponding values extracted from the USFS IW-FIA maps. Linear relationships were observed even where the RMSE filter was not applied, with the low correlation coefficients clearly at least partly a result of a relatively small number of outliers (Fig. 9a–c). After filtering for contamination, outliers, high RMSE on model fitting, and topographic shading, almost all of the outliers were removed (Fig. 9d–f). The following discussion pertains to the final data set.

The results of the comparison with reference data are summarized in Table 2. The mean absolute error in estimates of

fractional crown cover, mean canopy height, and woody biomass were 0.10, 2.2 m, and 4.5 ton acre⁻¹ (10.1 Mg ha⁻¹), with RMSE errors of 0.12, 3.3 and 6.2 (14.0), respectively. The relationships between retrieved and reference crown cover, canopy height and woody biomass were significant at the 99% level and could not have occurred by chance. A stronger relationship was found between estimated and reference biomass than for crown cover or mean canopy height ($R^2 = 0.81$). Error in the cover and height retrievals is normally distributed with no important bias. There is somewhat less dispersion at lower biomass values than at higher values. This may reflect the calibration of the background response using data from sparse canopies with shrubs, sub-shrubs and grasses; no attempt was made to recalibrate the relationships employed for more dense forest canopies. A certain degree of extrapolation error might therefore be expected, especially if the kernel weights are regarded as purely empirical descriptors of surface reflectance magnitude and anisotropy. In addition, the method for obtaining the background response in shrublands and grasslands is predicated on the assumption that the background accounts for a relatively high proportion of cover, since higher volume scattering effects are apparent when the understory is dense. Where the volume scattering effects from tree crowns overwhelm those of the understory, estimation of the background response may be compromised, although this does not appear to have had an important impact on the retrievals.

Estimates of fractional crown cover showed a strong relationship to the reference data ($R^2 = 0.78$) that was slightly weaker at higher cover values. This may again reflect extrapolation error in the estimation of the background response and the violation of the assumption of greater volume scattering effects with increasing understory cover. However, in general crown cover was overestimated, indicating that the understory estimation may not be the reason for the weaker relationship at high cover values. The estimates of mean canopy height demonstrate a slightly weaker linear relationship to the reference data than fractional crown cover or woody biomass ($R^2 = 0.69$). Canopy height is overestimated for a number of points in the low range and underestimated at higher values, reaching an asymptote at around 25 m (but for < 15 data points out of 576 in the final data set).

Retrieval accuracy depends on several factors, including remote sensing data integrity (here largely depending on atmospheric correction since MISR is well-calibrated), model appropriateness, landscape heterogeneity, smoothness of the error surface, sufficiency of the minimization algorithm, and the *a priori* estimates of the background response encapsulated in the empirical Walthall model. The last is particularly important when using GO models that account for the contributions of upper canopy and background elements separately in landscapes with sparse canopies. In spite of its simplicity, the model replicated MISR data over forest for a wide range of conditions without compromising inversion results. The implications of discarding the contributions from shaded crown and ground, following the derivation of the linear, semi-empirical, kernel-driven models, have not been pursued in this study. Although their impact is thought to be negligible, future work will examine whether including their contributions might improve retrievals.

Table 2
Error and correlation in the retrievals

	Fractional crown cover (dimensionless)	Mean canopy height (m)	Woody biomass (ton acre ⁻¹) (Mg ha ⁻¹)	
Mean relative error (%)	30	28	28	28
Mean absolute error	0.10	2.2	4.5	10.1
Mean (MISR)	0.48	10.3	21.8	49.0
Mean (USFS)	0.38	8.7	21.8	49.0
Root mean square error	0.12	3.3	6.2	14.0
R^2	0.78	0.69	0.81	0.81

Note: These error and correlation statistics were calculated with respect to the USFS IW-FIA data set that is based on remotely sensed data (MODIS) – along with other variables – in a modeling framework.

4. Conclusions

This study demonstrates the utility of multi-angle data for mapping woody plant cover, canopy height, and woody biomass over large areas. The objective was to access and exploit the canopy structural information encapsulated in the multiangle signal in MISR data through a GO modeling approach that attempts to assess the background contribution for each location *a priori*. Although important advances have been made previously in distinguishing between sparse and dense canopies by adjusting parameterized models against MISR data (Nolin, 2004; Pinty et al., 2002; Widlowski et al., 2004), to our knowledge this is the first time that data from a moderate resolution passive spaceborne remote sensing instrument have been used to map specific structural attributes of forest canopies over large areas in a canopy reflectance modeling framework in which plants are modeled as discrete objects. Note that only MISR data were used in the mapping approach presented here.

Model fits to MISR data were very good across all forested areas, whether upland or in river valleys. The quality of the model fitting to the MISR data (RMSE) was shown to be an important arbiter of retrieval accuracy: only when good fits were obtained did the prediction of these canopy parameters attain acceptable levels of accuracy. This is what would be expected where thin cloud, contrails, and other residual atmospheric contamination are not accounted for adequately by the atmospheric correction procedure: it appears to be possible to remove the residual contamination by merit of its impact on the directional signal. The possibility of the confounding of model parameters owing to their internal coupling in the model does not prohibit retrievals of fractional cover and crown shape, allowing calculation of mean canopy height and reasonable estimates of woody biomass.

This study has shown that the method is generalizable and that forest canopy structure information can be reliably retrieved from moderate resolution multiangle data over large areas. However, further tests of the accuracy of retrievals will be performed in the near future using ground reference rather than modeled data. A limitation of this study is that the reference data used were not intended for validation purposes: the FIA Interior West maps are draft data sets intended for review. Work is currently under way to provide a more thorough validation of the retrieved parameters using plot data from the FIA database. These data will also be useful in pursuing improved retrievals by allowing recalibration of the relationships used to obtain the background contribution. The relationships used here were obtained only in grass- and shrub-dominated areas in the USDA, ARS Jornada Experimental Range and the extrapolation of these relationships outside the domain in which they were obtained is a likely cause of inaccuracy. Nonetheless, we obtained good results over the extended domain and accuracy is expected to improve when new relationships for a range of forested areas become available.

The main advantage of the multiangle approach demonstrated here over active remote sensing methods is that it enables both timely and extensive estimates of key forest parameters at low cost. Regularly updated forest maps are valuable in mapping

stand age, timber volume, wildlife habitat, and disturbance. Assessments of gaseous (CO₂, CO) and particulate (aerosol) emissions from forest fires via estimates of biomass loss are likely to be more accurate than those from nadir-pointing passive instruments, since the vertical dimension is taken into account. Forest parameters retrieved using MISR data with a simple GO model might also prove useful when combined in a predictive modeling approach such as that used by the US Forest Service in its mapping work (e.g., Blackard & Moisen, 2005) alongside temporal-spectral remote sensing measures, or in a synergistic approach where data from active instruments are used to calibrate or train the passive multiangle observations (e.g., Kimes et al., 2006). The results reported here also show that the development of an operational MISR forest data product with utility in a wide range of mapping applications is feasible.

Acknowledgments

The MISR data were obtained from the NASA Langley Research Center Atmospheric Science Data Center. We thank David Diner (MISR Scientist, NASA/JPL) and the MISR Science Team; Ron Tymcio and Tracey Frescino (US Forest Service, Rocky Mountain Research Station, Ogden, UT); Michael White (Utah State University, Logan, UT); and Matt Smith and the Global Land Cover Facility (University of Maryland, College Park, MD). We are also extremely grateful to the four anonymous reviewers for their excellent observations and suggestions. This research was supported by NASA Earth Observing System grant NNG04GK91G managed under the NASA Land Cover Land Use Change program (manager: Dr. Garik Gutman). The Jornada Experimental Range, a NASA Land Validation Core Site, is administered by the USDA Agricultural Research Service and is also a Long Term Ecological Research site supported by the National Science Foundation (DEB 0080412).

References

- Blackard, J. A., & Moisen, G. G. (2005). Mapping forest attributes in the Interior Western states using FIA data, MODIS imagery and other geospatial layers. Research poster available at http://www.fs.fed.us/rm/ogden/research/posters/jblackard_SAF2005_100.pdf (last access: 11/01/06)
- Brent, R. P. (1973). Algorithms for function minimization without derivatives. Englewood Cliffs, NJ: Prentice-Hall.
- Chen, J. M., Li, X., Nilson, T., & Strahler, A. (2000). Recent advances in geometrical optical modeling and its applications. *Remote Sensing Reviews*, 18, 227–262.
- Chopping, M., Su, L., Laliberte, A., Rango, A., Peters, D. P. C., & Kollikkathara, N. (2006). Mapping shrub abundance in desert grasslands using geometric-optical modeling and multiangle remote sensing with CHRIS/Proba. *Remote Sensing of Environment*, 104(1), 62–73. doi:10.1016/j.rse.2006.04.022
- Chopping, M., Su, L., Rango, A., Martonchik, J. V., Peters, D. P. C., & Laliberte, A. (2008). Remote sensing of woody shrub cover in desert grasslands using MISR with a geometric-optical canopy reflectance model. *Remote Sensing of Environment*, 112, 19–34
- Diner, D. J., Asner, G. P., Davies, R., Knyazikhin, Y., Muller, J. -P., Nolin, A. W., et al. (1999). New directions in Earth observing: Scientific applications of multi-angle remote sensing. *Bulletin of the American Meteorological Society*, 80(11), 2209–2229.
- Diner, D. J., Braswell, B. H., Davies, R., Gobron, N., Hu, J., Jin, Y., et al. (2005). The value of multiangle measurements for retrieving structurally and

- radiatively consistent properties of clouds, aerosols, and surfaces. *Remote Sensing of Environment*, 97, 495–518.
- Disney, M., & Lafont, S. (2004). Comparison of MODIS VCF product with detailed ground-based inventory. Research poster for the *MODIS Vegetation Workshop*, 17–19 August 2004 USA: University of Montana available at <http://www.geog.ucl.ac.uk/~mdisney/publications.html> (last access: 10/29/06)
- Hansen, M. C., Defries, R., Townshend, J., Carroll, M., Dimiceli, C., & Sohlberg, R. (2003). Global percent tree cover at a spatial resolution of 500 meters: First results of the MODIS vegetation continuous fields algorithm. *Earth Interactions*, 7(10), 1–15.
- Kimes, D. S., Ranson, K. J., Sun, G., & Blair, J. B. (2006). Predicting lidar measured forest vertical structure from multi-angle spectral data. *Remote Sensing of Environment*, 100, 503–511.
- Li, X., & Strahler, A. H. (1985). Geometric–optical modeling of a conifer forest canopy. *IEEE Transactions on Geoscience and Remote Sensing*, 23, 705–721.
- Nilson, T., & Kuusk, A. (1989). A reflectance model for the homogenous plant canopy and its inversion. *Remote Sensing of Environment*, 27, 157–167.
- Nolin, A. W. (2004). Towards retrieval of forest cover density over snow from the Multi-angle Imaging SpectroRadiometer (MISR). *Hydrological Processes*, 18, 3623–3636.
- Pinty, B., Widlowski, J. -L., Gobron, N., Verstraete, M. M., & Diner, D. J. (2002). Uniqueness of multiangular measurements — Part I: An indicator of subpixel surface heterogeneity from MISR. *IEEE Transactions on Geoscience and Remote Sensing*, 40(7), 1560–1573.
- Powell, M. J. D. (1964). An efficient method for finding the minimum of a function in several variables without calculating derivatives. *Computer Journal*, 7, 155–162.
- Rahman, H., & Dedieu, G. (1994). SMAC: A simplified method for the atmospheric correction of satellite measurements in the solar spectrum. *International Journal of Remote Sensing*, 15, 123–143.
- Ross, J. K. (1981). *The radiation regime and architecture of plant stands*: The Hague: Dr. W. Junk Publishers, 392 pp.
- Roujean, J. -L., Leroy, M., & Deschamps, P. -Y. (1992). A bidirectional reflectance model of the Earth's surface for the correction of remote sensing data. *Journal of Geophysical Research*, 97(D18), 20455–20468.
- Ruefenacht, B., Moisen, G. G., & Blackard, J. A. (2004). Forest type mapping of the interior west. *Proceedings of the Tenth Forest Service Remote Sensing Applications Conference: Remote Sensing for Field Users*, Salt Lake City, Utah, April 5–9 2004.
- Running, S. W. (2006). Is global warming causing more, larger wildfires? *Science*, 313(5789), 927–928. doi:10.1126/science.1130370
- Strahler, A. H., Jupp, D. L. B., Woodcock, C. E., & Li, X. (2005). The discrete-object scene model and its application in remote sensing. *Proc. of the Intl. Symposium on Physical Measurements and Signature in Remote Sensing*, 2005, Beijing, China.
- Strahler, A. H., Wanner, W., Schaaf, C., Li, X., Hu, B., Muller, J. -P., et al. (1996). MODIS BRDF/albedo product: Algorithm theoretical basis documentation, Version 4.0. NASA/EOS ATBD 94 pp.
- US Forest Service (2005). Interior West FIA Geospatial Products — 2005 IW-FIA metadata document available at http://www.fs.fed.us/rm/ogden/map-products/intwest/map_pdfs/iw_models_2005_metadata.pdf (latest access 11/01/06)
- Walthall, C. L., Norman, J. M., Welles, J. M., Campbell, G., & Blad, B. L. (1985). Simple equation to approximate the bidirectional reflectance from vegetative canopies and bare surfaces. *Applied Optics*, 24, 383–387.
- Wanner, W., Li, X., & Strahler, A. H. (1995). On the derivation of kernels for kernel-driven models of bidirectional reflectance. *Journal of Geophysical Research*, 100, 21077–21090.
- Westerling, A. L., Hidalgo, H. G., Cayan, D. R., & Swetnam, T. W. (2006). Warming and earlier spring increases Western U.S. forest wildfire activity. *Science*, 313(5789), 940–943. doi:10.1126/science.1128834
- White, M. A., Shaw, J. D., & Ramsey, R. D. (2005). Accuracy assessment of the vegetation continuous field tree cover product using 3954 ground plots in the south-western USA. *International Journal of Remote Sensing*, 26(12), 2699–2704.
- Widlowski, J. -L., Pinty, B., Gobron, N., Verstraete, M., Diner, D. J., & Davis, B. (2004). Canopy structure parameters derived from multi-angular remote sensing data for terrestrial carbon studies. *Climatic Change*, 67, 403–415.